

COMPRESSIVE STRENGTH VARIATION OF CONCRETE SPECIMENS DUE TO IMPERFECTION SENSITIVITY

K. Ikeda,
Department of Civil Engineering, Tohoku University, Sendai, Japan
K. Maruyama,
Department of Civil Engineering, Nagaoka University of Technology
Nagaoka, Japan

Abstract

On the basis of the standpoint of bifurcation, the stochastic variation of compressive strength of cylindrical concrete specimens is ascribed with the variation of initial imperfections of the specimens. The explicit formula of the probability density function of the compressive strength and several pertinent power laws for imperfection sensitivity are employed to testify that concrete specimens under compression do indeed undergo bifurcation.

1 Introduction

Compressive strength of concrete specimens is well known to suffer a statistical variation. It is customary to ascribe such a variation to variations of material properties, such as, the frictions at the boundaries and the grading and arrangement of aggregates.

In an earlier stage of the research, the statistical variation was examined based on the experiment on more than 100 concrete specimens, for example, by Cusens and Wettern (1959). Owing to a lack of a firm theoretical basis, the normal distribution is often employed to simulate the histogram of the compressive strength.

“Fracture” due to distributed cracking is acknowledged as a potential cause of the compressive failure of concrete, in addition to

other brittle materials, such as rocks and metals. Bažant (1983, 1984), for example, extensively investigated the fundamental mechanism of the failure and size effect of concrete due to fracture.

By contrast, in the field of soil mechanics, “bifurcation” has come to be acknowledged as a major source of shear failure. Vermeer (1982), for example, performed a shear band analysis of granular materials, as an extension of the plastic bifurcation by Hill and Hutchinson (1975). Ikeda and Goto (1993) employed the concept of imperfection sensitivity to develop a method to assess the presence of bifurcation for sand specimens, and demonstrated the mechanism of a size effect in specimen height. This method serves as an extension of the Koiter law (1945) and the bifurcation equation by Thompson and Hunt (1973). Furthermore, Ikeda et al. (1995) explained the variation of the shear strength of sand specimens by combining this method with a theory of the stochasticity of initial imperfections by Ikeda and Murota (1993).

The aim of this paper is to explain the stochastic variation of the load versus displacement curves and the maximum loads of an ensemble of cylindrical concrete specimens based on the standpoint of bifurcation. With the use of the major assumption that these specimens undergo bifurcation, such variation is ascribed with the variation of initial imperfections among specimens. The theory of the stochasticity is employed to obtain the explicit formula of the probability density function of the compressive strength. Experimental data are shown to accurately follow several pertinent power laws for imperfection sensitivity (Ikeda and Goto, 1993), which offer information on bifurcation of concrete specimens. Further we simulate the load versus displacement curves by means of the bifurcation equation. The present method has successfully simulated and categorized the behavioral characteristics of various kinds of concrete specimens, and hence to insure the major assumption that the concrete specimens do undergo bifurcation.

2 Bifurcation Theory

In this section we offer a summary of Ikeda and Murota (1993) and Ikeda and Goto (1993) as a basic tool to represent the mechanism of strength variation of specimens based on the standpoint of bifurcation. We consider a system of nonlinear equilibrium equations

$$\mathbf{H}(P, \mathbf{u}, \mathbf{v}) = \mathbf{0}, \quad (1)$$

where P denotes a loading parameter (axial stress in this paper);

\mathbf{u} indicates a nodal displacement (or position) vector; and \mathbf{v} an imperfection vector. We assume H to be sufficiently smooth.

For a fixed \mathbf{v} , a set of solutions (P, \mathbf{u}) of the above system of equations (1) makes up equilibrium paths. Fig. 1 illustrates typical behavior in the vicinity of a bifurcation point (P_c^0, \mathbf{u}_c^0) of the perfect system shown as (o). Here the dashed lines stand for the paths for the perfect system, the solid ones for the imperfect one, and (●) for a limit point (P_c, \mathbf{u}_c) of the imperfect system, governing the maximum stress (critical load) of the specimen (structure). Here $(\cdot)_c$ refers to the critical point and $(\cdot)^0$ to the perfect system. A critical point, which is either a bifurcation or limit point, is defined as a point where the Jacobian of the system becomes singular, that is, $\det \partial \mathbf{H} / \partial \mathbf{u} = 0$. Such point is categorized into simple, double, and so on, according to the number of zero eigenvalues of the Jacobian is equal to 1, 2, \dots .

We write

$$\mathbf{v} = \mathbf{v}^0 + \epsilon \mathbf{d}, \quad P_c = P_c^0 + \delta P_c, \quad (2)$$

where $\epsilon (\geq 0)$ denotes the magnitude of the initial imperfection ($\epsilon = 0$ for a perfect system and $\epsilon > 0$ for an imperfect one); \mathbf{d} is a vector indicating the pattern of initial imperfections; and δP_c means the increment of the critical load. The analyses presented in the sequel are all asymptotic and are valid only when ϵ is small.

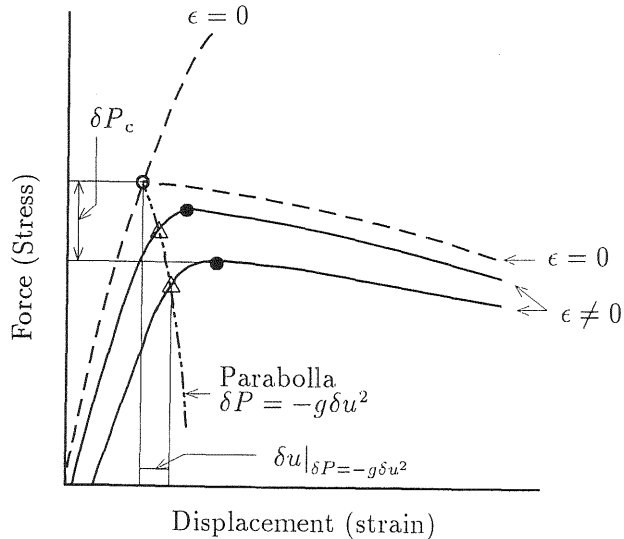


Fig. 1 Force-displacement curve in the vicinity of a bifurcation point

In the vicinity of an unstable simple symmetric bifurcation point or an unstable double ¹ bifurcation point, the Koiter law (1945) relates the increment (decrease) δP_c of the maximum stress (critical load) P_c for an imperfect system with the magnitude ϵ of initial imperfections, that is,

$$\delta P_c = P_c - P_c^0 \sim C_0 a^{2/3} \epsilon^{2/3} \quad (3)$$

Here C_0 is a constant, and the explicit form of the variable $a = a(\mathbf{d})$, which is dependent on the type of critical points, is given in Murota and Ikeda (1991)

The law in Eq. (3) gives information only on the maximum stress. For the simple symmetric bifurcation point, Ikeda and Goto (1993) derived a more general imperfection sensitivity law for an arbitrary displacement, say $u \equiv u_i$. It is to be emphasized here that all the results given below are applicable also for the double point ². First by taking the difference between the equilibrium equations (1) for the bifurcation point (P_c^0, \mathbf{u}_c^0) of the perfect system and for the limit point (P_c, \mathbf{u}_c) for the imperfect one, and by eliminating the displacements other than u , we can obtain:

$$(\delta u - r\delta P - s\delta u^2)\delta P + p(\delta u - r\delta P - s\delta u^2)^3 + q\epsilon + \text{h.o.t.} = 0, \quad (4)$$

which denotes the incremental force δP versus displacement δu curve for the perfect system for $\epsilon = 0$ and for imperfect one for $\epsilon \neq 0$. Here p, q, r and s are some constants, and $\delta u \equiv u - u_c^0$ denotes the incremental displacement for an arbitrary displacement component $u \equiv u_i$ from the bifurcation point for the perfect system.

Next we consider the parabola

$$\delta P = -g\delta u^2, \quad (5)$$

shown by the dotted-dashed line in Fig. 1 (g is a positive constant). The substituting of Eq. (5) into Eq. (4) and the omitting of the terms higher than δu^3 lead to

$$\delta u|_{\delta P = -g\delta u^2} \sim \left(\frac{q}{g-p}\right)^{1/3} \epsilon^{1/3}, \quad (6)$$

¹As a double point, we consider only the group-theoretic unstable double bifurcation point of an axisymmetric system the index of which is greater than five [see Ikeda, Murota, and Fujii (1991) for details].

²Such applicability is based on the fact that the bifurcation equation for the double bifurcation point can be reduced to that for the simple symmetric bifurcation point through a simple transformation. See, e.g., Murota and Ikeda (1991).

where $\delta u|_{\delta P = -g\delta u^2}$ denotes the displacement on the intersection point [shown as (Δ) in Fig. 1] of the parabola $\delta P = -g\delta u^2$ and an imperfect P versus u curve.

Finally the combination of Eqs. (3) and (6) yields a power law

$$\delta P_c \sim D(\delta u|_{\delta P = -g\delta u^2})^2, \quad (7)$$

which is pertinent to testify the presence of bifurcation based on experimental force versus displacement (stress versus strain) curves. Here $D = C_0[a(g-p)/q]^{2/3}$ is a constant.

In order to investigate the stochastic properties of buckling loads P_c , let us consider the case where the imperfection pattern vector \mathbf{d} is subject to a multivariate normal distribution with a mean $\mathbf{0}$ and with a positive definite variance-covariance matrix W^{-1} . We focus on the double bifurcation point in the remainder of this paper [see Ikeda and Murota (1993) for the results for other types]. The probability density function of the critical load P_c is evaluated to

$$f_{P_c}(P_c) = \frac{3(P_c - P_c^0)^2}{2C^3} \exp\left(\frac{-|P_c - P_c^0|^3}{2C^3}\right), \quad -\infty < P_c < P_c^0, \quad (8)$$

where C is a constant associated with the variance. The mean $E[P_c]$ and the variance $\text{Var}[P_c]$ of P_c are expressed respectively as

$$E[P_c] = P_c^0 - 1.13C, \quad \text{Var}[P_c] = (0.409C)^2. \quad (9)$$

It is to be emphasized here that by the present method a mere calculation of the sample mean $E[P_c]$ and variance $\text{Var}[P_c]$ of the critical loads will yield the values of parameters P_c^0 and C in Eq. (9), and, in turn, the probability density function in Eq. (8).

3 Application

We have carried out a series of compression tests on cylindrical concrete specimens under the same condition to obtain two sets of axial stress-axial strain ($\sigma - \varepsilon$) curves shown in Fig. 2. Aggregates were obtained from the Shinano river: aggregate size was 2.5-5.0 (mm) for Case A (13 specimens) and 10-15 (mm) for Case B (13 specimens). These specimens had a constant diameter of 10 cm and a height of 20 cm. Ordinary Portland cement was used. The curves in Fig. 2 are investigated in the sequel by means of the present method in §2, which hold also for this case merely by replacing

$$P \rightarrow \sigma, \quad u_i \rightarrow \varepsilon.$$

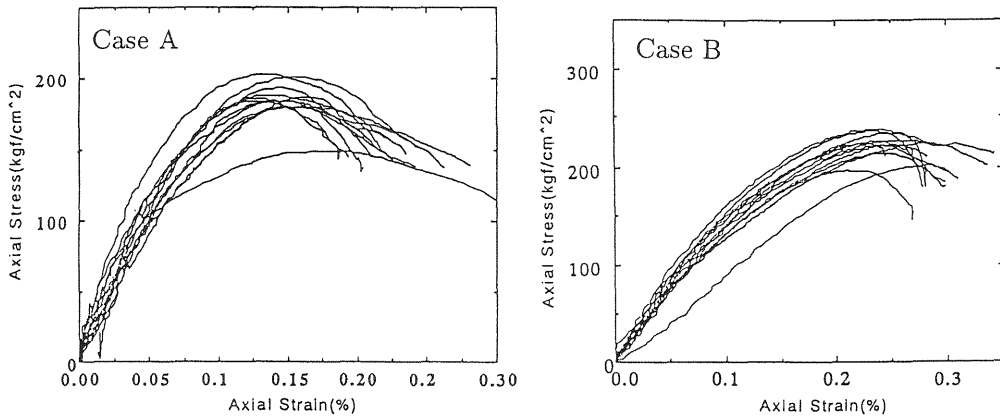


Fig. 2 Stress versus strain curves for concrete specimens

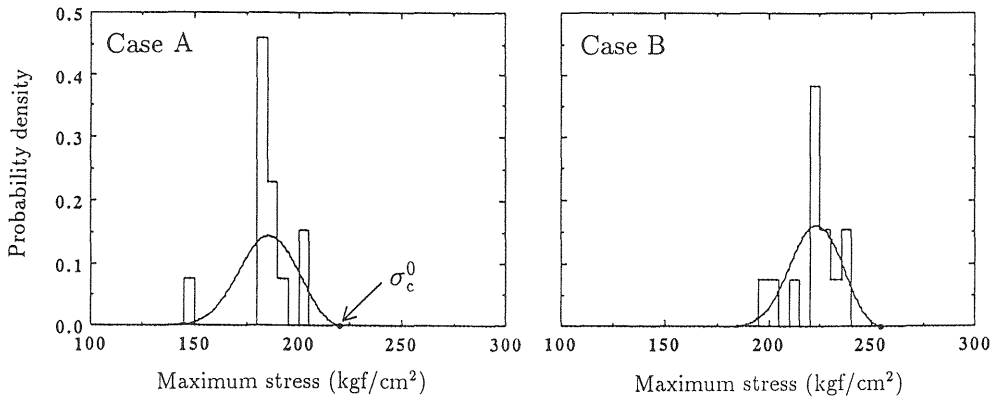


Fig. 3 Histogram and probability density function of maximum stress

Table 1 Estimated values of σ_c^0 and C

	$E_{\text{sample}}[\sigma_c]$ (kgf/cm ²)	$\text{Var}_{\text{sample}}[\sigma_c]$ (kgf ² /cm ⁴)	σ_c^0 (kgf/cm ²)	C (kgf/cm ²)
Case A	184.9	173.3	221.0	32.2
Case B	222.5	140.4	255.0	29.0

Fig. 3 shows the histogram of the maximum stress σ_c for those specimens. The use of the sample mean $E_{\text{sample}}[\sigma_c]$ and the sample variance $\text{Var}_{\text{sample}}[\sigma_c]$ of the maximum stress σ_c in Eq. (9) led to the values of σ_c^0 and C listed in Table 1. The substitution of these values into Eq. (8) led to the probability density function of σ_c shown by the solid curves in Fig. 3. Although the difference between these curves and the histograms may appear to be large, such difference will be reduced by increasing the number of specimens. It is noteworthy that the curves are bounded rightward at the critical stress ratio σ_c^0 for the perfect system, because σ_c for imperfect systems cannot exceed σ_c^0 for whatever initial imperfections.

In order to assess the validity of the power law in Eq. (7), we first obtained the intersection point of the parabola $\delta\sigma = -g\delta\varepsilon^2$ (see Fig. 1) and the experimental σ versus ε curves shown in Fig. 3. Fig. 4 shows interrelationships between $\delta\sigma_c$ and the square of the incremental displacement $\delta\varepsilon|_{\delta\sigma=-g\delta\varepsilon^2}$ for this point. Here the values of g and ε_c^0 , which are listed in Table 2, were chosen in such a manner that the power law in Eq. (7) correlated accurately with the experiment; at the course of this it was noted that this correlation was sensitive not to g but to ε_c^0 . This agrees with the nature of Eq. (7), which holds for any g and the true ε_c^0 . The straight line in this figure denotes the least square approximation of the experimental data. It is, in particular for Case A, fairly in good accordance with the linear relationship between $\delta\sigma_c$ and $(\delta\varepsilon|_{\delta\sigma=-g\delta\varepsilon^2})^2$ of Eq. (7) that should pass the origin. This assesses the validity of the present procedure to explain the variation of soil shearing behavior by the “stochasticity of initial imperfections.”

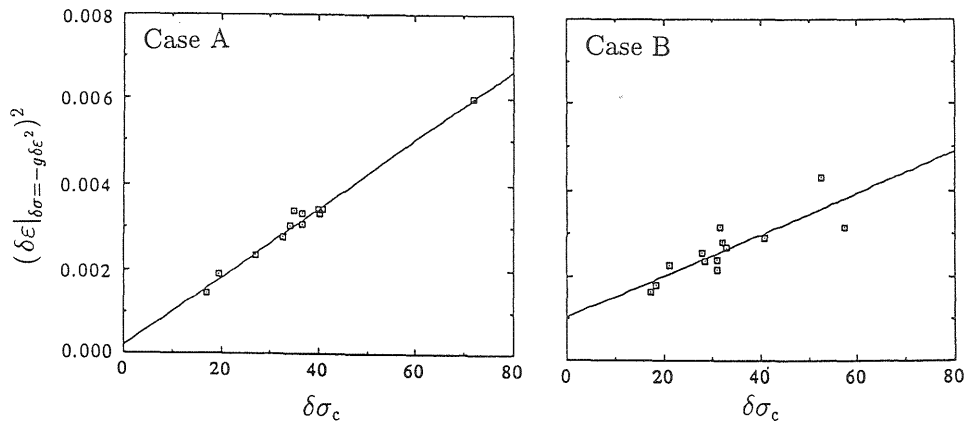


Fig. 4 Experimental $\delta\sigma_c - (\delta\varepsilon|_{\delta\sigma=-g\delta\varepsilon^2})^2$ relationships

The simulation of the representative sets of experimental stress-strain ($\sigma - \varepsilon$) curves by the theoretical curves in Eq. (4) is shown in Fig. 5. Here the parameters p , q , r and s in Eq. (4) were chosen based on preliminary analyses. The theoretical curves shown by the dashed lines correlate fairly well with the experimental ones by the solid ones.

Table 2 Values of parameters for asymptotic simulation
(unit in kgf and cm)

	ε_c^0	g	p	q	r	s
Case A	0.08	1.2×10^4	1.6×10^3	0.83	3.8×10^{-4}	1.0×10^{-6}
Case B	0.16	1.8×10^4	6.9×10^2	1.07	7.5×10^{-4}	1.0×10^{-6}

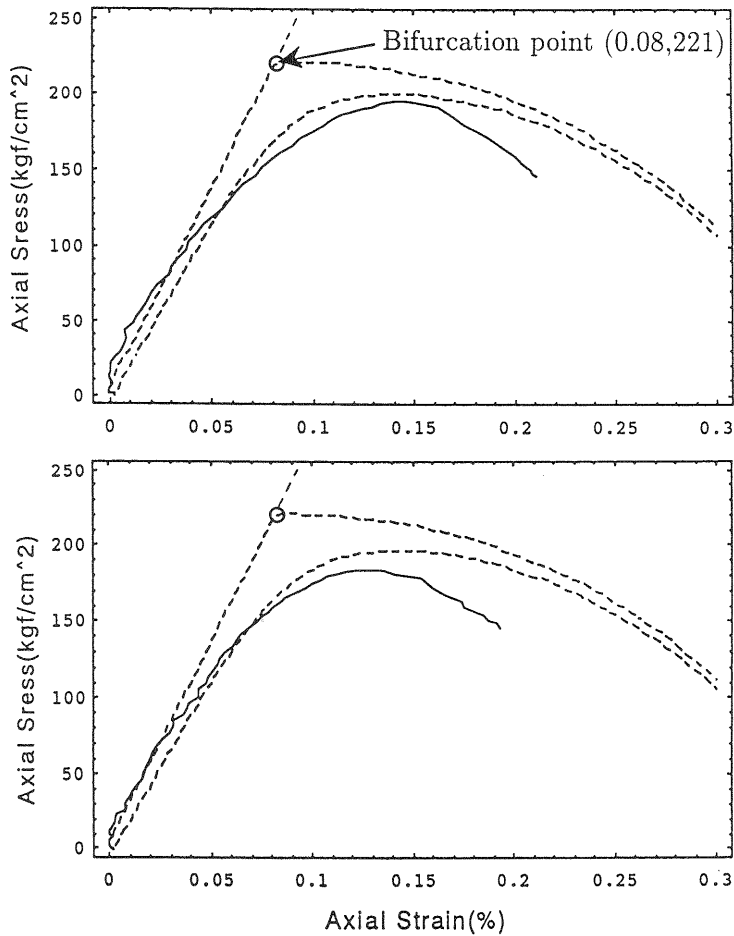


Fig. 5 Simulation of stress-strain ($\sigma - \varepsilon$) curves (Case A)

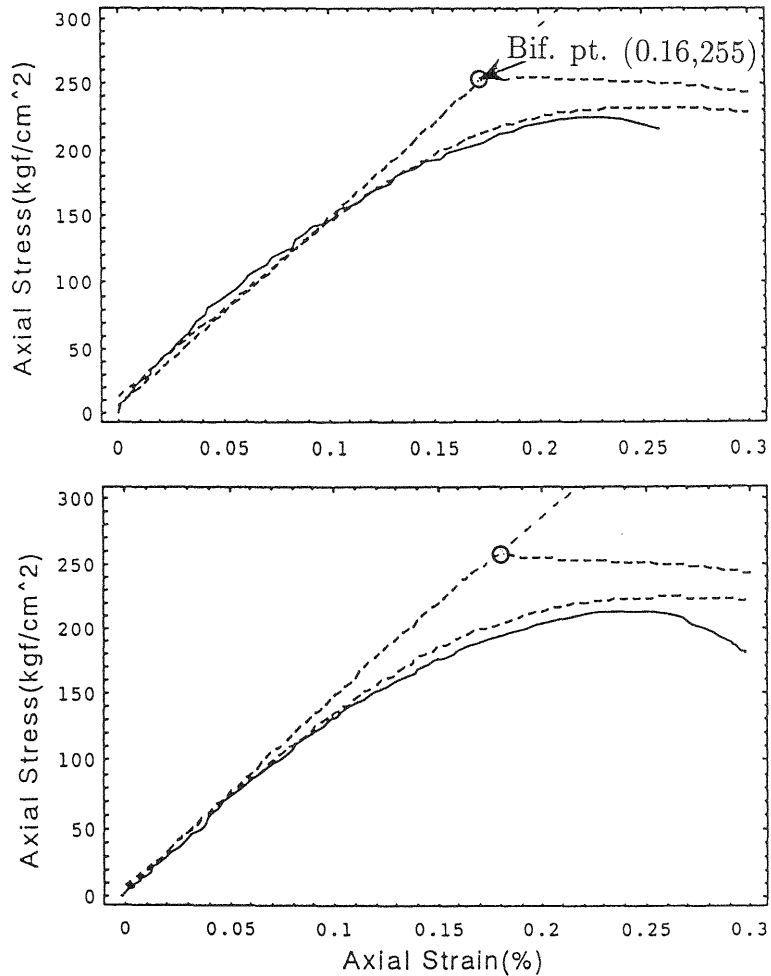


Fig. 5 Simulation of stress-strain ($\sigma - \varepsilon$) curves (Case B)

4 Conclusions

The various formulas presented in §2 can explain well the various aspects of the compressive behavior of the concrete specimens. This shows the validity and usability of the present method. It may be ironical that one can extract important information on bifurcation from the probabilistic variation of the compressive strength that is indeed problematic in experiments.

5 Acknowledgement

The authors would like to thank for Mr. Ishida and Kagawa for their ardent support in the experiment and analysis. This research was supported by the grant number 06805038 of the Japanese Ministry of Education.

6 References

- Bažant, Z.P. (1983) Fracture in concrete and reinforced concrete, in **IUTAM Prager Symp. Mech. Geomaterials: Rocks, Concrete, Soils** (ed. Z.P. Bažant), Northwestern University, 281–316.
- Bažant, Z.P. (1984) Size effect in blunt failure: concrete, rock, metal. **J. Eng. Mech., ASCE**, 110(4), 518–535.
- Cusens, A.R. and Wettern, J.H. (1959) Quality control in factory-made precast concrete. **Civil Eng. & Public Works Rev.**, 54.
- Hill, R. and Hutchinson, J.W. (1975) Bifurcation phenomena in the plane tension test. **J. Mech. & Phys. Solids**, 23, 239–264.
- Ikeda, K., Chida, T. and Yanagisawa, E. (1995) Imperfection sensitive strength variation of soil specimens. Preprint.
- Ikeda, K. and Goto, S. (1993) Imperfection sensitivity for size effect of granular materials. **Soils & Foundations**, 33(2), 157–170.
- Ikeda, K. and Murota, K. (1993) Statistics of normally distributed initial imperfections. **Int. J. Solids & Structures**, 30(18), 2445–2467.
- Koiter, W.T. (1945) On the stability of elastic equilibrium, **Dissertation. Delft, Holland**, (English translation: NASA Tech. Trans. F10: 833, 1967).
- Murota, K. and Ikeda, K. (1991) Critical imperfection of symmetric structures. **SIAM J. Applied Math.**, 51(5), 1222–1254.
- Thompson, J.M.T. and Hunt, G.W. (1973) **A General Theory of Elastic Stability**. John Wiley and Sons, New York.
- Vermeer, P.A. (1982) A simple shear-band analysis using compliances. **IUTAM, Conf. Deformation & Failure Granular Materials**, 493–499.